Electronic Supplementary Material (ESI) for Physical Chemistry Chemical Physics.
This journal is © the Owner Societies 2017

Electronic Supplementary Information for

Evidence for Cooperative Na^+ and Cl^- Binding by Strongly Hydrated L-Proline

Olga A. Dmitrieva,[a] Marina V. Fedotova,[a*] and Richard Buchner[b*]

[a]G. A. Krestov Institute of Solution Chemistry, Russian Academy of Sciences,
Akademicheskaya st. 1, 153045 Ivanovo, Russia

[b]Institut für Physikalische und Theoretische Chemie, Universität Regensburg,
93040 Regensburg, Germany

---

[*] To whom correspondence should be addressed; E-mail: hebrus@mail.ru, Richard.Buchner@chemie.uni-regensburg.de

1 Methods — Statistical Mechanics

For 1D-RISM site-specific coordination numbers, $n_{\alpha\beta}$, were obtained from radial pair distribution functions (PDFs), $g_{\alpha\beta}(r)$, as

$$n_{\alpha\beta} = 4\pi\rho_\beta \int_0^{r_{\min}} g_{\alpha\beta}(r) r^2 \, \mathrm{d}r \tag{S1}$$

where ρ_β is the average number density of solvent sites/atoms of kind β. Such partial coordination numbers give the average number of sites/particles of type β in a coordination sphere of radius $r_{\min}$ around an α site. The integration limit, $r_{\min}$, is defined by the position of the first minimum of the PDF and corresponds to the radius of the first coordination shell around reference site α.

In the case of 3D-RISM the spatial distribution functions (SDFs), $g_\beta(\boldsymbol{r})$, give the spatial distribution of solvent molecules around a solute molecule, which is commonly represented by isodensity surfaces at a selected probability level (see Fig. 6 of the main manuscript). From such SDFs the associated total coordination number of sites β within a shell of volume V_s in contact with the reference molecule can be calculated as

$$n_\mathrm{t} = \rho_\beta \int_0^{V_\mathrm{s}} g_\beta(\boldsymbol{r}) \, \mathrm{V} \tag{S2}$$

Since Pro is not a spherical molecule, its hydration shell is also not spherical. Thus, for the calculation of the total water coordination number the previously suggested approximation for the first hydration shell as a closed surface with arbitrary shape was used.[1]

The SDFs can also be used to calculate cylindrical distribution functions (CDFs), $g_{\mathrm{pyr}-\alpha}(z)_R$, originally derived for describing the local atom density adjacent to planar surfaces of molecules.[2] These CDFs give the probability of finding a specific site at a distance, z, orthogonal to the reference plane xy defined by the central molecule, within a cylinder of radius R.[1,3] For the present investigation such CDFs are a useful tool to characterize the distribution of water molecules above and below the plane of the pyrrolidine ring and to calculate corresponding coordination numbers, see Fig. S1.

2 Methods — Correction for kinetic depolarization

Due to their electric field ions orient surrounding solvent dipoles to some extent. When moving in an external electric field, $\vec{E}$, ions therefore exert a torque on surrounding solvent dipoles opposing the tendency of the latter to align with $\vec{E}$. This purely dynamical effect, with a finite magnitude at zero frequency, leads to a depolarization of the bulk solvent in addition to solvation effects and accordingly, the experimentally detected bulk-water amplitude, S_b, is reduced by the kinetic dielectric decrement, $\Delta\varepsilon_\mathrm{kd}$, compared to the equilibrium amplitude, S_b^eq, reached in the absence of ionic motion.[4] The latter is also reduced compared to the pure solvent because of solvent dilution and, mainly, ion solvation.[5] In electrolytes of salt concentration c the amplitude relevant for calculating the DRS-detected concentration of bulk-like solvent, c_b, and thus of the total effective solvation number, Z_t, is therefore given by

$$S_\mathrm{b}^\mathrm{eq}(c) = S_\mathrm{b}(c) + \Delta\varepsilon_\mathrm{kd} \tag{S3}$$

The original continuum theory of Hubbard and Onsager[4] (HO) was derived for vanishing salt concentration and thus is problematic when correcting experimental S_b values but recently Sega *et al.*[6] published a phenomenological modification valid also at finite salt concentrations, yielding

$$\Delta\varepsilon_\mathrm{DD} = p \times \frac{\varepsilon_\mathrm{w}(0) - \varepsilon_\infty(0)}{\varepsilon_\mathrm{w}(0)} \times \tau_\mathrm{w}(0) \times \frac{\kappa}{\varepsilon_0} \times \exp[-\kappa_\mathrm{D} R] \times (\kappa R + 2)/2 \tag{S4}$$

where $\varepsilon(0)\,[= 78.368]$ is the static permittivity of the pure solvent, $\varepsilon_\infty(0)\,[= 3.52]$ is the infinite-frequency permittivity, $\tau_\mathrm{w}(0)\,[= 8.35\,\mathrm{ps}]$ its relaxation time, κ is the solution conductivity, ε_0 the electric field constant and κ_D the reciprocal Debye length.[7] For the effective ion size $R = (r_+ + d_\mathrm{w} + r_-)/2 = 0.284\,\mathrm{nm}$ was chosen, where r_+ and r_- are the radii of Na^+ and Cl^-, and d_w is the diameter of a water molecule.[8] For the hydrodynamic parameter the value for slip boundary conditions, $p = 2/3$, was chosen as this yielded consistent limiting ionic hydration numbers when used with HO theory for vanishing electrolyte concentrations.[5]

3 Supplementary Tables

Table S1: Site-specific coordination numbers, $n_{\alpha\beta}$, and corresponding distances, $r_{\alpha\beta}$ (in brackets), of L-proline in aqueous solutions as a function of Pro concentrations, c(Pro), from 1D-RISM calculations

c(pro) / M	0^a	1.0	2.0	3.0	4.0	5.0	6.0
Carboxylate group							
n_{O1Ow}	7.95	7.24	6.49	6.14	5.50	5.06	4.43
(r_{O1Ow} / nm)	(0.310)	(0.310)	(0.310)	(0.310)	(0.310)	(0.310)	(0.310)
n_{O2Ow}	7.10	6.48	5.82	5.56	4.98	4.57	3.94
(r_{O2Ow} / nm)	(0.313)	(0.313)	(0.313)	(0.313)	(0.313)	(0.313)	(0.310)
n_{O1Hw}	2.21	2.13	2.05	1.98	1.87	1.77	1.66
(r_{O1Hw} / nm)	(0.175)	(0.175)	(0.175)	(0.175)	(0.175)	(0.175)	(0.175)
n_{O2Hw}	1.90	1.82	1.73	1.68	1.61	1.52	1.41
(r_{O2Hw} / nm)	(0.178)	(0.178)	(0.178)	(0.178)	(0.178)	(0.178)	(0.178)
NH_2^+ group							
n_{N1Ow}	4.48	4.23	3.94	3.69	3.40	3.14	2.84
(r_{N1Ow} / nm)	(0.300)	(0.298)	(0.298)	(0.298)	(0.298)	(0.295)	(0.295)
n_{H8Ow}	0.90	0.87	0.82	0.78	0.75	0.70	0.65
(r_{H8Ow} / nm)	(0.175)	(0.175)	(0.175)	(0.175)	(0.175)	(0.175)	(0.175)
n_{H9Ow}	0.83	0.79	0.75	0.70	0.66	0.62	0.57
(r_{H9Ow} / nm)	(0.173)	(0.170)	(0.170)	(0.170)	(0.170)	(0.170)	(0.170)
Ring carbon atoms							
n_{C2Ow}	3.88	3.77	3.49	3.13	2.87	2.64	2.37
(r_{C2Ow} / nm)	(0.340)	(0.338)	(0.338)	(0.338)	(0.338)	(0.335)	(0.335)
n_{C3Ow}	5.44	5.31	4.94	4.50	4.14	3.84	3.49
(r_{C3Ow} / nm)	(0.355)	(0.355)	(0.355)	(0.353)	(0.350)	(0.350)	(0.350)
n_{C4Ow}	6.68	6.37	5.97	5.64	5.38	5.01	4.59
(r_{C4Ow} / nm)	(0.350)	(0.350)	(0.348)	(0.348)	(0.348)	(0.345)	(0.345)
n_{C5Ow}	6.96	6.60	6.15	5.80	5.36	4.97	4.51
(r_{C5Ow} / nm)	(0.323)	(0.323)	(0.323)	(0.323)	(0.320)	(0.320)	(0.320)
H_2O sandwiching pyrrolidine ring[b]							
$n_{\mathrm{pyr-Ow}}$	1.04	0.98	0.93				0.56
Hydrophilic sites: $n_\mathrm{h} = n_{\mathrm{O1Ow}} + n_{\mathrm{O2Ow}} + n_{\mathrm{N1Ow}}$							
n_h	19.53	17.95	16.25	15.39	13.88	12.77	11.21
Total number of first-shell H_2O molecules, n_t (3D-RISM)							
n_t	25.4	24.0	22.4				13.2

[a] Data for hydrophilic sites taken from Fedotova and Dmitrieva[9]; [b] from CDF peaks at $z = 0.360$ nm (6M: 0.340 nm) and –0.340 nm, see Fig. S1.

Table S2: 1D-RISM results for site-specific coordination numbers, $n_{\alpha\beta}$, and corresponding distances, $r_{\alpha\beta}$ (in brackets), of L-proline in aqueous Pro+NaCl solutions of $c(\mathrm{Pro}) = 0.6\,\mathrm{M}$, and $c(\mathrm{NaCl})$

$c(\mathrm{NaCl})\,/\,\mathrm{M}$	0	0.2	0.5	1.0	1.5	2.0
Carboxylate group						
n_{O1Ow}	7.43	7.44	7.35	7.27	7.20	7.12
$(r_{\mathrm{O1Ow}}\,/\,\mathrm{nm})$	(0.310)	(0.310)	(0.310)	(0.310)	(0.310)	(0.310)
n_{O2Ow}	6.65	6.67	6.60	6.53	6.49	6.42
$(r_{\mathrm{O2Ow}}\,/\,\mathrm{nm})$	(0.313)	(0.313)	(0.313)	(0.313)	(0.313)	(0.313)
n_{O1Hw}	2.12	2.11	2.09	2.06	2.04	2.01
$(r_{\mathrm{O1Hw}}\,/\,\mathrm{nm})$	(0.175)	(0.175)	(0.175)	(0.175)	(0.175)	(0.175)
n_{O2Hw}	1.83	1.82	1.80	1.77	1.75	1.73
$(r_{\mathrm{O2Hw}}\,/\,\mathrm{nm})$	(0.178)	(0.178)	(0.178)	(0.178)	(0.178)	(0.178)
NH_2^+ group						
n_{N1Ow}	4.31	4.28	4.23	4.16	4.11	4.04
$(r_{\mathrm{N1Ow}}\,/\,\mathrm{nm})$	(0.298)	(0.298)	(0.298)	(0.298)	(0.298)	(0.300)
n_{H8Ow}	0.87	0.86	0.85	0.84	0.82	0.81
$(r_{\mathrm{H8Ow}}\,/\,\mathrm{nm})$	(0.175)	(0.175)	(0.175)	(0.175)	(0.175)	(0.175)
n_{H9Ow}	0.79	0.79	0.77	0.76	0.74	0.73
$(r_{\mathrm{H9Ow}}\,/\,\mathrm{nm})$	(0.170)	(0.170)	(0.170)	(0.173)	(0.173)	(0.173)
Ring carbon atoms						
n_{C2Ow}	3.91	3.88	3.85	3.80	3.63	3.58
$(r_{\mathrm{C2Ow}}\,/\,\mathrm{nm})$	(0.340)	(0.340)	(0.340)	(0.340)	(0.340)	(0.340)
n_{C3Ow}	5.46	5.27	5.39	5.33	5.29	5.23
$(r_{\mathrm{C3Ow}}\,/\,\mathrm{nm})$	(0.353)	(0.353)	(0.353)	(0.353)	(0.353)	(0.353)
n_{C4Ow}	6.51	6.48	6.42	6.34	6.30	6.23
$(r_{\mathrm{C4Ow}}\,/\,\mathrm{nm})$	(0.350)	(0.350)	(0.350)	(0.350)	(0.350)	(0.350)
n_{C5Ow}	6.72	6.68	6.61	6.51	6.45	6.36
$(r_{\mathrm{C5Ow}}\,/\,\mathrm{nm})$	(0.323)	(0.323)	(0.323)	(0.323)	(0.323)	(0.323)
Hydrophilic sites: $n_{\mathrm{h}} = n_{\mathrm{O1Ow}} + n_{\mathrm{O2Ow}} + n_{\mathrm{N1Ow}}$						
n_{h}	18.39	18.39	18.18	17.96	17.80	17.58
Na^+-carboxylate interactions						
n_{O1Na}			0.04			0.14
$(r_{\mathrm{O1Na}}\,/\,\mathrm{nm})$			(0.258)			(0.258)
Cl^--NH_2^+ group interactions						
n_{H8Cl}			0.02			0.08
$(r_{\mathrm{H8Cl}}\,/\,\mathrm{nm})$			(0.188)			(0.188)
n_{H8Cl}			0.02			0.0.08
$(r_{\mathrm{H8Cl}}\,/\,\mathrm{nm})$			(0.183)			(0.183)

4 Supplementary Figures

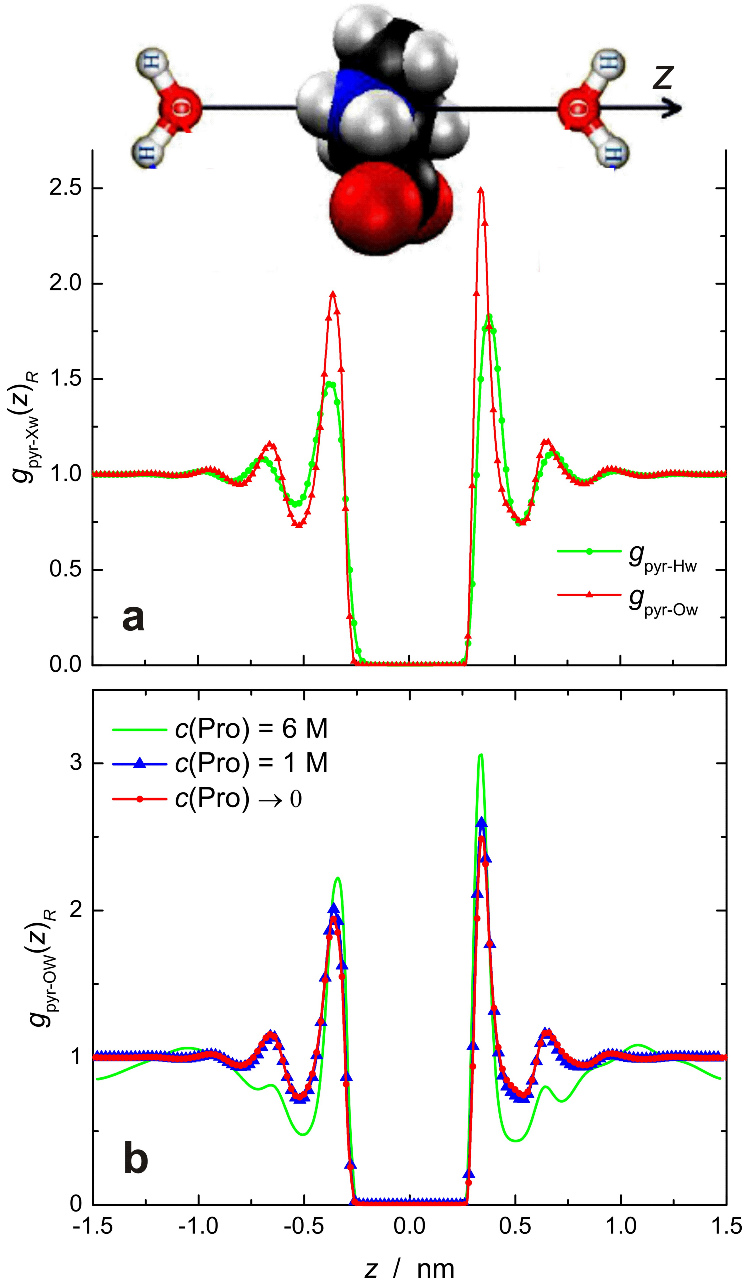

Figure S1: (a) Cylindrical distribution functions, $g_{\mathrm{pyr-Ow}}(z)_R$ and $g_{\mathrm{pyr-Hw}}(z)_R$ ($R = 0.126\,\mathrm{nm}$), for H_2O hydrating the pyrrolidine ring of Pro at $c(\mathrm{Pro}) \to 0$; (b) Concentration dependence of $g_{\mathrm{pyr-Ow}}(z)_R$ for aqueous L-proline solutions.

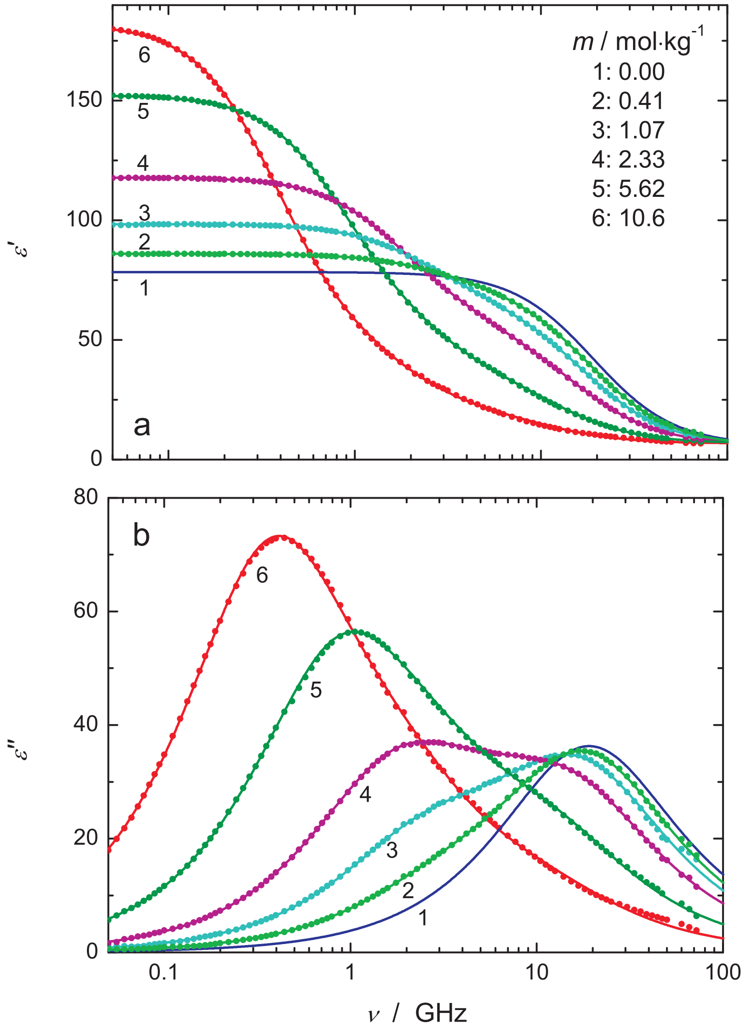

Figure S2: Spectra of (a) relative permittivity, $\varepsilon'(\nu)$, and (b) dielectric loss, $\varepsilon''(\nu)$, of aqueous L-proline solutions at 25 ℃ and concentrations $c(\mathrm{Pro})\,/\,\mathrm{M} = 0$ (1), 0.395 (2), 0.981 (3), 1.944 (4), 3.805 (5), 5.569 (6). Symbols show experimental data, the lines give fits with the D+D+D model.

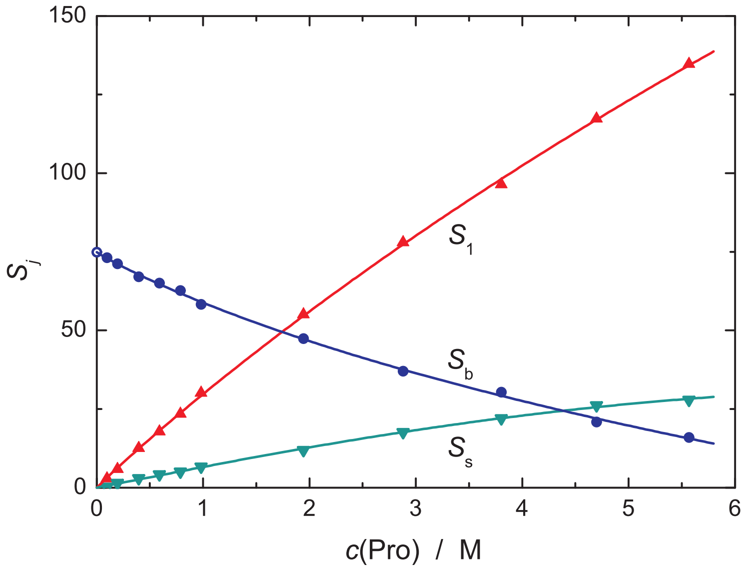

Figure S3: Relaxation amplitudes of the solute mode, S_1 (▲), of slow water, $S_s = S_2$ (▼), and of bulk-like water, S_b (●) of aqueous L-proline solutions at 25 ℃ and solute concentrations c(Pro). Lines are guide to the eye; the open symbol is pure water.

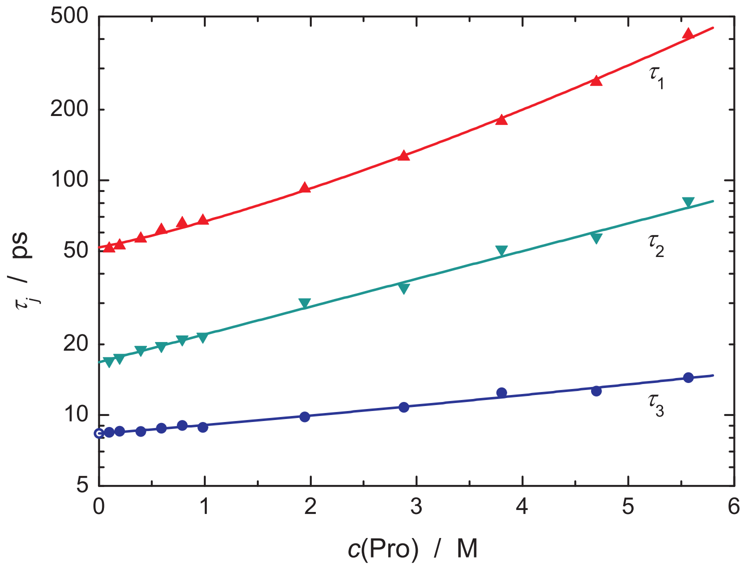

Figure S4: Relaxation times of the solute mode, τ_1 (▲), of slow water, $\tau_s = \tau_2$ (▼), and of the cooperative relaxation of bulk-like water, τ_3 (●) of aqueous L-proline solutions at 25 ℃ and solute concentrations c(Pro). Lines are guide to the eye; the open symbol is pure water.

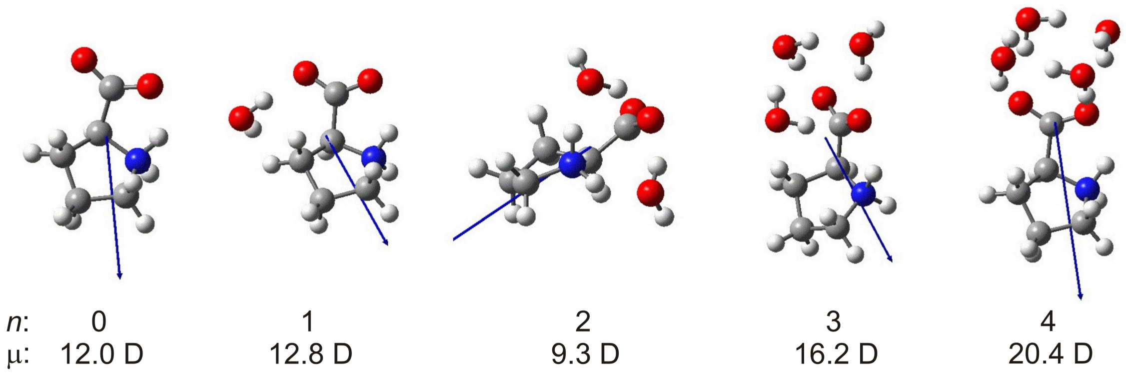

Figure S5: Minimum-energy structures of Pro·nH$_2$O ($n = 0 \dots 4$) complexes and their associated dipole moments, μ, obtained with Gaussian (B3LYP/cc-pVDZ level with C-PCM solvation model).[10,11] The arrow indicates the dipole direction.

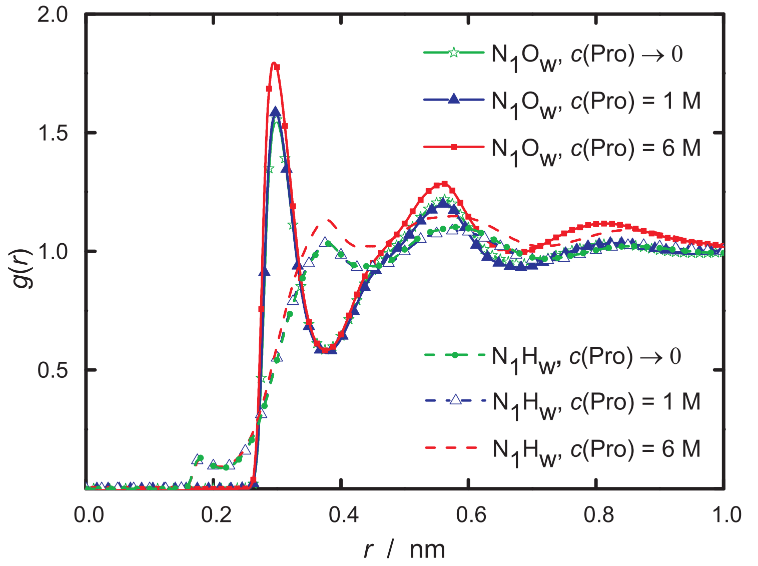

Figure S6: Pair distribution functions $g_{\mathrm{N1Ow}}(r)$ (solid lines) and $g_{\mathrm{N1Hw}}(r)$ (broken lines) of aqueous L-proline solutions at 25 ℃.

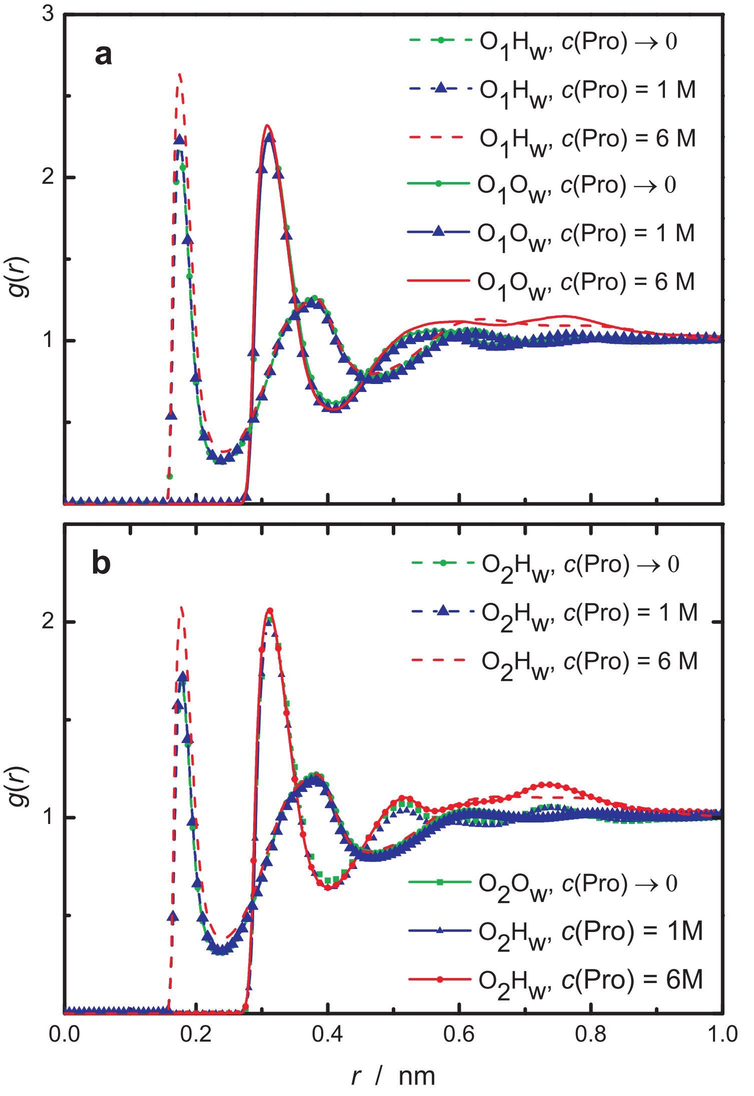

Figure S7: (a) Pair distribution functions $g_{\mathrm{O1Ow}}(r)$ (solid lines) and $g_{\mathrm{O1Hw}}(r)$ (broken lines) of aqueous L-proline solutions at 25 ℃. (b) Corresponding functions $g_{\mathrm{O2Ow}}(r)$ (solid lines) and $g_{\mathrm{O2Hw}}(r)$ (broken lines).

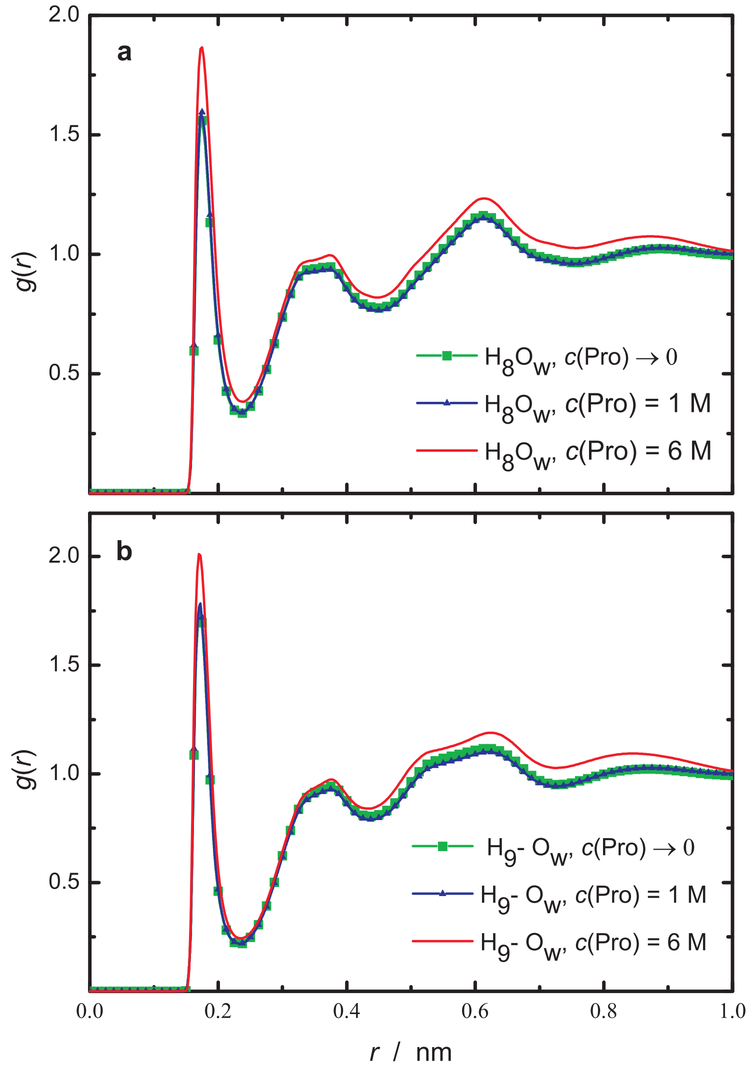

Figure S8: Pair distribution functions $g_{\mathrm{H8Ow}}(r)$ (a) and $g_{\mathrm{H9Ow}}(r)$ (b) of aqueous L-proline solutions at 25 ℃.

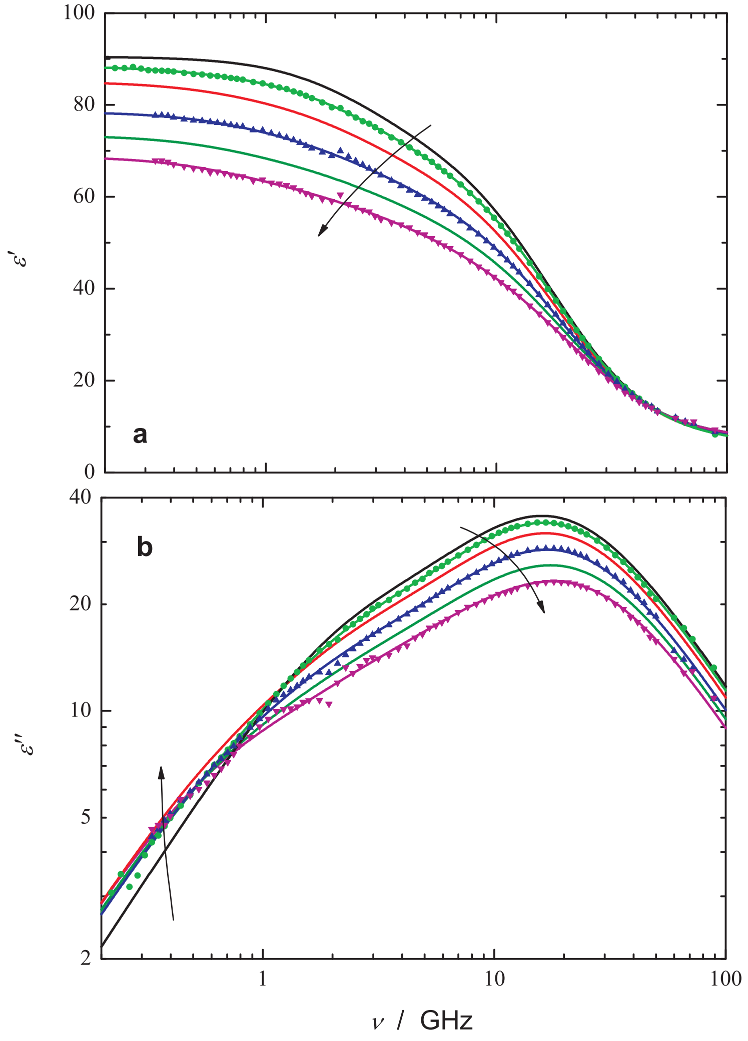

Figure S9: Spectra of (a) relative permittivity, $\varepsilon'(\nu)$, and (b) dielectric loss, $\varepsilon''(\nu)$, of solutions of NaCl in 0.6 M aqueous L-proline at 25 ℃ and concentrations $c(\mathrm{NaCl})\,/\,\mathrm{M} = 0$, 0.205, 0.999, 1.513, 2.023 increasing in arrow direction. Symbols show experimental data (partly omitted for clarity), the lines give fits with the D+D+D+D model.

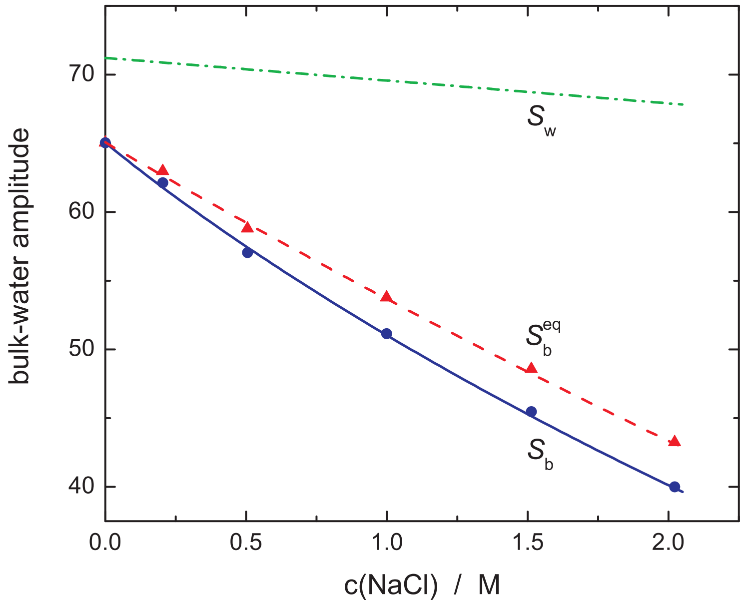

Figure S10: Experimental bulk-water amplitude, S_b (●), and corresponding equilibrium amplitude after correction for kinetic depolarization, S_b^{eq} (▲), of NaCl solutions of concentration c(NaCl) in 0.6 M aqueous L-proline at 25 ℃. Also included is the amplitude, S_w, expected from the analytical water concentration. The difference $S_w - S_b^{eq}$ yields the total concentration of bound water.

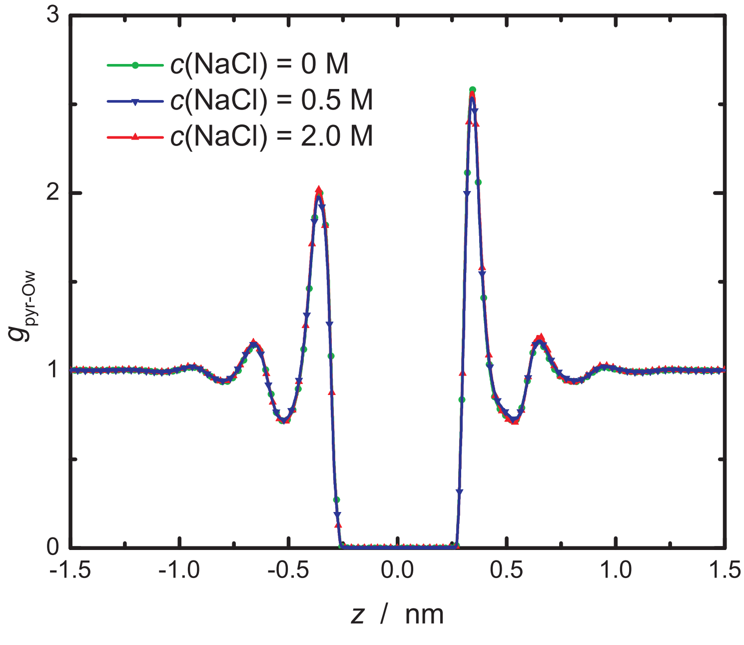

Figure S11: Cylindrical distribution functions, $g_{\mathrm{pyr-Ow}}(z)_R$ ($R = 0.126\,\mathrm{nm}$), for H_2O hydrating the pyrrolidine ring of Pro at $c(\mathrm{Pro}) = 0.6\,\mathrm{M}$ and $c(\mathrm{NaCl}) = (0,\ 0.5\ \mathrm{and}\ 2.0)\,\mathrm{M}$.

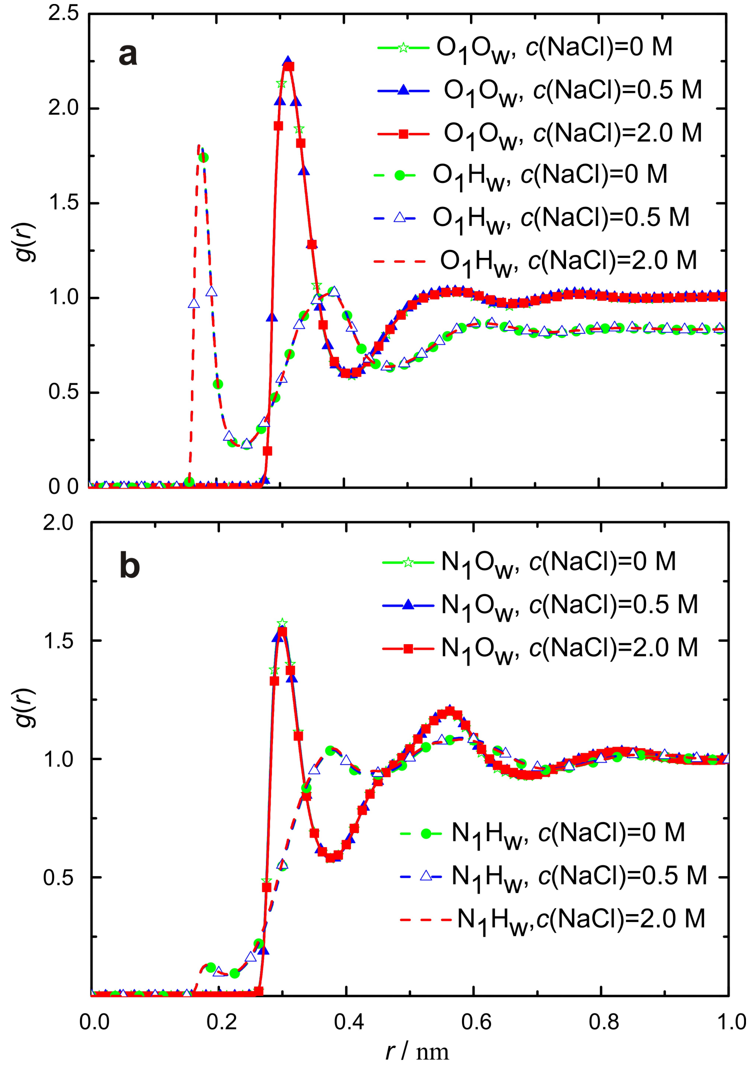

Figure S12: (a) Pair distribution functions $g_{\mathrm{O1Ow}}(r)$ (solid lines) and $g_{\mathrm{O1Hw}}(r)$ (broken lines) of NaCl solutions in 0.6 M aqueous L-proline at 25 ℃. (b) Corresponding functions $g_{\mathrm{N1Ow}}(r)$ (solid lines) and $g_{\mathrm{N1Hw}}(r)$ (broken lines).

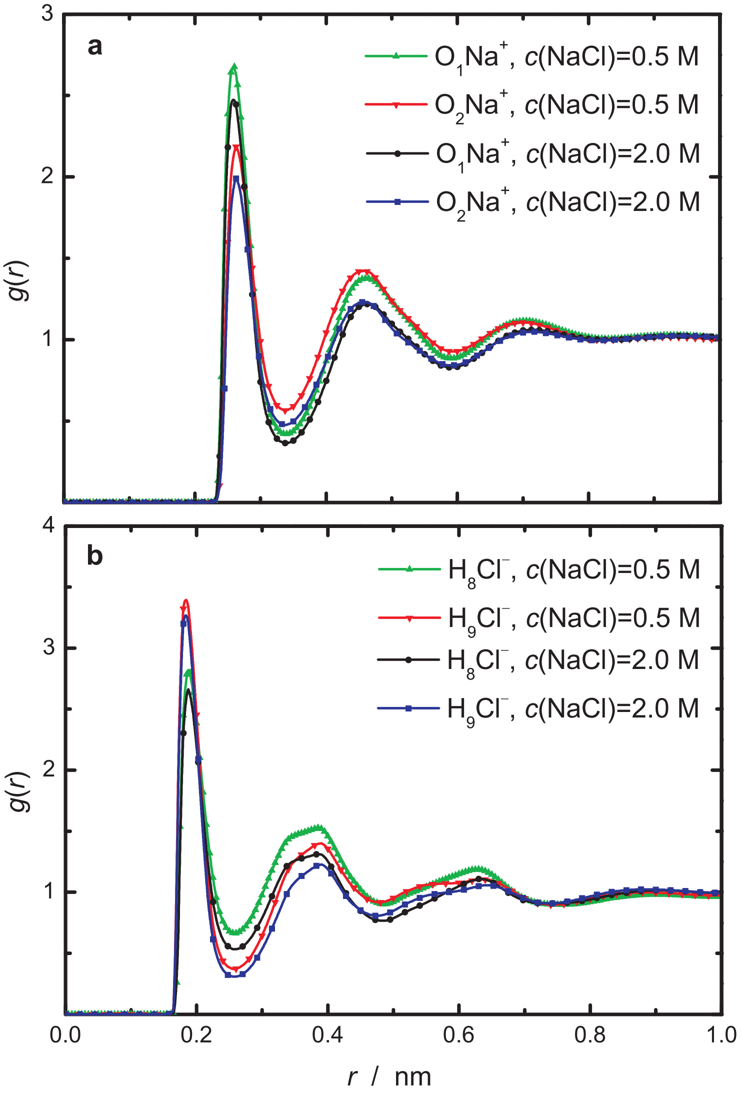

Figure S13: (a) Pair distribution functions $g_{\mathrm{O1Na}}(r)$ and $g_{\mathrm{O2Na}}(r)$ of 0.5 M and 2.0 M NaCl in 0.6 M aqueous L-proline at 25 ℃. (b) Corresponding functions $g_{\mathrm{H8Cl}}(r)$ and $g_{\mathrm{H9Cl}}(r)$.

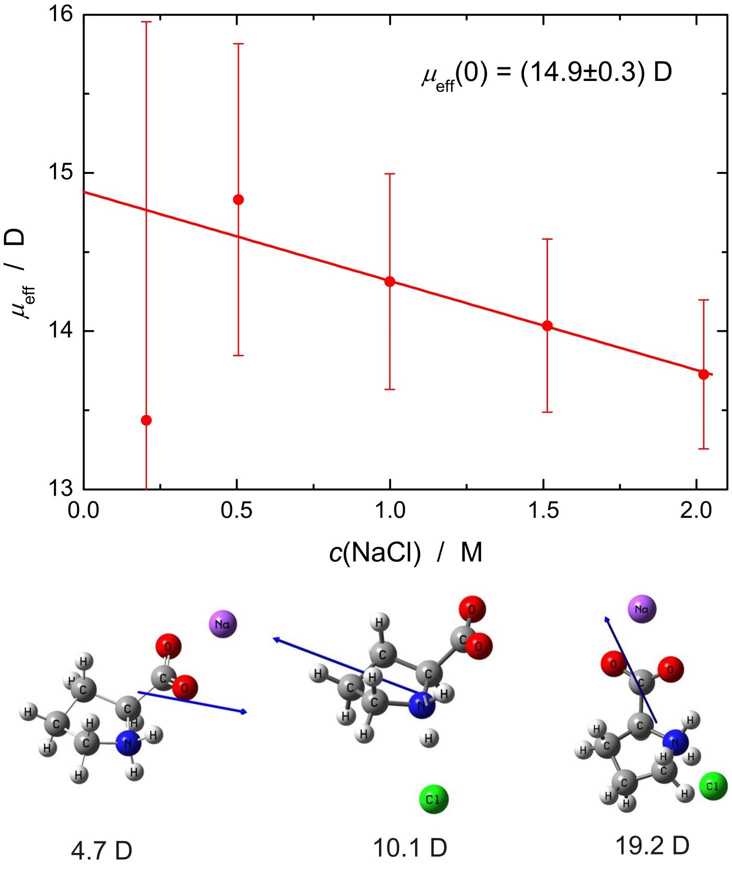

Figure S14: Effective dipole moment, μ_{eff} (●), of L-proline-ion aggregates as a function of NaCl concentration, c(NaCl), in 0.6 M L-proline(aq) at 25 °C obtained from the experimental amplitude S_1 corrected for ion-cloud relaxation. Also shown are the minimum-energy structures of pro·Na$^+$, pro·Cl$^-$ and pro·NaCl aggregates and their dipole moments obtained with Gaussian (B3LYP/cc-pVDZ level with C-PCM solvation model).[10,11] The arrow indicates the dipole direction.

References

[1] M. V. Fedotova and S. E. Kruchinin, *J. Mol. Liq.*, 2013, **179**, 27–33.

[2] A. Plugatyr, I. Nahtigal and I. M. Svishchev, *Chem. Phys.*, 2006, **124**, 024507–024515.

[3] M. V. Fedotova and S. E. Kruchinin, *J. Mol. Liq.*, 2013, **186**, 90–97.

[4] (*a*) J. B. Hubbard and L. Onsager, *J. Chem. Phys.*, 1977, **67**, 4850–4857; (*b*) J. B. Hubbard, *J. Chem. Phys.*, 1978, **68**, 1649–1664; (*c*) J. B. Hubbard, P. Colonomos and P. G. Wolynes, *J. Phys. Chem.*, 1979, **71**, 2652–2661.

[5] R. Buchner and G. Hefter, *Phys. Chem. Chem. Phys.*, 2009, **11**, 8984–8999.

[6] M. Sega, S. Kantorovich and A. Arnold, *Phys. Chem. Chem. Phys.*, 2015, **17**, 130–133.

[7] J. O. Bockris and A. K. N. Reddy, *Modern Electrochemistry*, Plenum, New York, 2nd edn, 1998, vol. 1.

[8] Y. Marcus, *Ion Properties*, Wiley, Chichester, 1997.

[9] M. V. Fedotova and O. A. Dmitrieva, *Russ. J. Phys. Chem. A*, 2014, **88**, 794–797.

[10] M. J. Frisch, G. W. Trucks, H. B. Schlegel, G. E. Scuseria, M. A. Robb, J. R. Cheeseman, G. Scalmani, V. Barone, B. Mennucci, G. A. Petersson, H. Nakatsuji, M. Caricato, X. Li, H. P. Hratchian, A. F. Izmaylov, J. Bloino, G. Zheng, J. L. Sonnenberg, M. Hada, M. Ehara, K. Toyota, R. Fukuda, J. Hasegawa, M. Ishida, T. Nakajima, Y. Honda, O. Kitao, H. Nakai, T. Vreven, J. Montgomery, J. A., J. E. Peralta, F. Ogliaro, M. Bearpark, J. J. Heyd, E. Brothers, K. N. Kudin, V. N. Staroverov, R. Kobayashi, J. Normand, K. Raghavachari, A. Rendell, J. C. Burant, S. S. Iyengar, J. Tomasi, M. Cossi, N. Rega, J. M. Millam, M. Kiene, J. E. Knox, J. B. Cross, V. Bakken, C. Adamo, J. Jaramillo, R. Gomperts, R. E. Stratmann, O. Yazyev, A. J. Austin, R. Cammi, C. Pomelli, J. W. Ochterski, R. L. Martin, K. Morokuma, V. G. Zakrzewski, G. A. Voth, P. Salvador, J. J. Dannenberg, S. Dapprich, A. D. Daniels, O. Farkas, J. B. Foresman, J. V. Ortiz, J. Cioslowski and D. J. Fox, *Gaussian 09, Revision B.01*, Gaussian Inc.: Wallingford CT, 2010.

[11] M. Cossi, N. Rega, G. Scalmani and V. Barone, *J. Comput. Chem.*, 2003, **24**, 669–681.